Friction **9**(2): 367–379 (2021)
https://doi.org/10.1007/s40544-020-0377-0
ISSN 2223-7690
CN 10-1237/TH
RESEARCH ARTICLE

Determination of coefficients of friction for laminated veneer lumber on steel under high pressure loads

Michael DORN[1,*], **Karolína HABROVÁ**[2], **Radek KOUBEK**[3], **Erik SERRANO**[4]

[1] *Department of Building Technology, Linnaeus University, Växjö 35252, Sweden*

[2] *Czech University of Life Sciences Prague-Department of Materials and Engineering Technology, Prague 16521, Czech Republic*

[3] *Daikin UK, The Heights, Brooklands, Weybridge, KT13 0NY, United Kingdom*

[4] *Division of Structural Mechanics, Lund University, Lund 22100, Sweden*

Received: 22 November 2018 / Revised: 28 September 2019 / Accepted: 24 February 2020

Abstract: In this study, static coefficients of friction for laminated veneer lumber on steel surfaces were determined experimentally. The focus was on the frictional behaviors at different pressure levels, which were studied in combination with other influencing parameters: fiber orientation, moisture content, and surface roughness. Coefficients of friction were obtained as 0.10–0.30 for a smooth steel surface and as high as 0.80 for a rough steel surface. Pressure influenced the measured coefficients of friction, and lower normal pressures yielded higher coefficients. The influence of fiber angle was observed to be moderate, although clearly detectable, thereby resulting in a higher coefficient of friction when sliding perpendicular rather than parallel to the grain. Moist specimens contained higher coefficients of friction than oven-dry specimens. The results provide realistic values for practical applications, particularly for use as input parameters of numerical simulations where the role of friction is often wrongfully considered.

Keywords: laminated veneer lumber (LVL); wood; static friction; high pressure; angle-to-grain; moisture content

1 Introduction

Friction is experienced in our daily activities, and its presence is typically unnoticed compared to its absence, for example, in slippery walkways or roads. However, in engineering practice, particularly in mechanical engineering, friction causes significant wear of machinery parts or higher energy consumption. Therefore, reducing friction using appropriate methods, such as suitable lubrication or surface treatments, is often desirable.

Although friction is encountered regularly in structural timber engineering, it is not considered explicitly in design. It occurs in conventional connections between the members (e.g., tenon joints) and in connections with metal fasteners (e.g., dowel-type connections or nails). Hirai et al. [1] reported effects of friction in timber constructions.

The influence of dowel roughness (frictional behavior between the dowel and the surrounding wood) has been studied experimentally, and high variation of the load-bearing behavior and ultimate loads has been observed [2, 3]. The influence of friction on the connection behavior is obtained by numerical simulations. Parametric studies clearly show the increase in contact area when high friction dowels are used and the failure mode is changed from splitting owing to wedge action towards shear failure in the surrounding wood [3, 4].

Frictional coefficients, 0.00 [5], 0.50 [6, 7], and 0.70

* Corresponding author: Michael DORN, E-mail: michael.dorn@lnu.se

Nomenclature

F_h	Horizontal force in the biaxial test set-up	μ	Coefficient of friction
F_v	Vertical force in the biaxial test set-up	μ_f	Coefficient of static friction
α	Angle between wood fiber direction and the applied pressure	μ_s	Coefficient of sliding friction

[8], are used frequently in numerical simulations of dowel-type connections. Because the friction coefficients clearly influence the results, the use of practical coefficients is essential (refer studies on the influence on dowel-type connections in Refs. [6] and [2]). However, currently, no comprehensive study on frictional coefficients has been performed, which could have been used for those types of applications.

Laminated veneer lumber (LVL) was used as the wood material in this study. LVL is an engineered wood product made from veneers of spruce (Picea abies) or pine (Pinus sylvestris) with 3 mm thickness that are glued by a phenol adhesive. A strong homogenization effect applies; that is, defects in the stem from, e.g., knots, are distributed evenly. The resulting product with a defined orientation shows excellent mechanical properties and a significantly improved form-stability as compared to structural lumber. Hence, lengthy beams and plates of stabilized quality and of larger cross-sectional dimensions can be produced. Therefore, LVL is widely used in structural timber engineering.

The present work provides an overview of influencing parameters on the frictional behaviors through experimental evidence.

1.1 Literature review

The frictional behaviors of wood, including static and sliding friction, have been studied previously. Dynamic coefficients of friction are important in paper manufacturing process when the wood is grinded or cut. Tool wear is critical to reduce the cost for replacement and maintenance. Additionally, energy consumption is influenced by the efforts in the processes. During the grinding process in paper production, wet conditions are commonly encountered, at room or elevated temperatures. In the building sector, static friction is the primary focus, which has been examined in previous studies. In the case of seismic action, sliding friction may be crucial.

The earliest study on determining static friction between steel surfaces mentioned in this study was performed by Atack and Tabor in the 1950s on Balsa wood (Abies balsamica) [9]. The tangential force is split into an interfacial part, from adhesion of two surfaces, and a deforming part, where softer material undergoes deformation due to the shearing. The samples were prepared in a way to remove even fats and acids from the surfaces, increasing reproducibility but limiting the practicality for applications.

The cutting of wood and the forces encountered are investigated by Klamecki [10]. The surface roughness is considered as the major parameter for friction to enable a linear relation between normal and friction forces for well-finished tools (adhesion of the surfaces as the major force). Tools with high surface roughness indicate high friction forces, whereby the asperities of the tools cut into the wood surfaces (known as plowing-type friction).

Murase studied wood friction in several studies, e.g., the effects of steel and other metals, including glass and various plastics in Ref. [11], both for static and dynamic friction.

Pressure levels of 0.1 and 0.6 MPa were applied by Möhler and Herröder on a large variety of combinations of wood and other materials (steel, concrete, and timber) [12]. Depending on the roughness of the steel surface, friction values for static friction between 0.5 and 1.2 were reported (at a rather high moisture content of 20%–25%), and dynamic friction was determined as well.

Coefficients of friction were determined for spruce wood by Möhler and Maier for use cases within timber engineering (such as curved beams or perpendicularly pre-stressed connections with bolts) [13]. Coefficients of friction of wood on wood were found to increase with moisture content and decrease with applied pressure. Rough-sawn surfaces had clearly higher

values (approximately 0.49 and 0.93 for wood with moisture content of 10%–17% and >30%, respectively) than planed surfaces (approximately 0.30 and 0.81 for wood with 10%–20% and >30% moisture content, respectively).

McKenzie found decreasing values of sliding friction with increased moisture content of wood on different steel surfaces [14] and additionally stated that friction coefficients varied slightly with fiber angle without any further explanation.

A study by Bejo, et al. reported a decrease in friction coefficients with applied contact pressure for the range of 0.5–60 kPa in a non-linear manner [15]. Tests conducted through an inclined plane method on yellow-poplar LVL yielded static friction coefficients between 0.63 and 0.37 along the grain and 0.70 and 0.40 across the grain.

Kuwamura obtained a clear decrease in the static coefficient of friction, particularly for coarse steel surfaces, with an increase in normal pressure [16]. Coarse steel surface exhibited higher coefficients than fine surfaces, whereby exhibiting approximately identical friction coefficients at high pressure levels. Other studies have reported decreasing coefficients of friction with increased applied pressure for all directions [17]. Seki et al. reported the behavior for the tangential and radial directions, but not for the longitudinal direction [18].

1.2 Test methods

There are various methods to determine friction behaviors (often assessed together with wear). The ASTM G 115-10 [19] provides a detailed overview of these methods.

Static coefficients of friction for wood materials have traditionally been analyzed using an inclined or a horizontal plane method, as can be found in several of the above-cited publications. In the first case, which is a simple method, the angle of an inclined plane to the horizontal plane is measured at the point where the test specimen starts sliding. In the second case, the specimen is put flat onto the sliding plane, and a horizontal force is applied to move the specimen. Wood species, annual ring orientation, steel surface properties, or moisture content can be varied easily with both variants.

In the inclined plane method, the pressure in the shear plane cannot be controlled easily due to the consideration of the dead weight. However, in the horizontal plane method, some extra weight can be put onto the specimen for additional force. Similarly, here the applied pressure in the sliding plane is limited due to practical reasons.

When friction under high pressure levels is studied, different and more sophisticated methods should be employed to allow controlled test conditions. Forces, as encountered in this test series, were as high as approximately 30 kN to apply up to 35 MPa compressive stress on the test specimens (at an area of approx. 30 mm × 30 mm). The test method is explained in the subsequent sections.

1.3 Objectives

The objective of this work is to present coefficients of static friction for LVL on steel surfaces. A multitude of parameters are varied to quantify their influences on the coefficients of friction. Particularly, the influence of pressure in the sliding plane is analyzed.

2 Experimental details

Frictional tests require a set-up allowing for a controlled application and measurement of the forces and deformations, particularly when high normal forces are applied. Moreover, the test specimens and the surfaces must be manufactured with high precision to enable uniform distribution of the loads over the surface. The materials and methods used in this investigation are presented in the following subsections. First, the test set-up and the machinery are described, followed by descriptions of the tested variations, and then the preparation and conditioning of the wood specimens. Finally, the test and evaluation procedures are described.

2.1 Test set-up

A biaxial test machine was used to apply high force in the vertical and horizontal (sliding) directions. An MTS 322-based test frame machine was employed for precise and highly accurate control and measurement of the deformations and forces encountered. Figure 1 shows the test machine with the mounted

test rig. Parts 1 and 7 are the fixed parts from the test machinery between which the set-up is mounted. Part 1 is the vertically moving crosshead, and part 7 is the horizontal sledge. Part 6, which is basically a rigid spacer screwed tightly onto the sledge (part 7), is the lower loading device that transfers the force from bottom to top. The fixture (part 5) is mounted onto the lower loading device and enables insertion of different mounting plates (parts 4a–4c). The test specimen is fixed onto those plates (part 3). On top, the exchangeable sliding plate (part 2) is screwed to the upper cross head (part 1) via an intermediate distance plate.

A critical point in the design of the test set-up is the mounting of the specimens. Mounting should be done in an accurate, simple, and quick way. In addition, high forces must be introduced safely without destroying the specimen prematurely before sliding. Therefore, the specimens were assembled on a mounting plate with a highly structured surface finish (part 4c). During the application of the vertical loads, the teeth in the mounting plate are pressed into the specimen to establish a mechanical connection. This ensures that the horizontal loads can be transferred without failure in this plane, even for the tests with a rough steel plate (which was not ensured when a less structured mounting plates was used (part 4a)). Additionally, minimal time is required for specimen change as compared to gluing the specimens to a separate mounting plate (part 4b), which is time consuming.

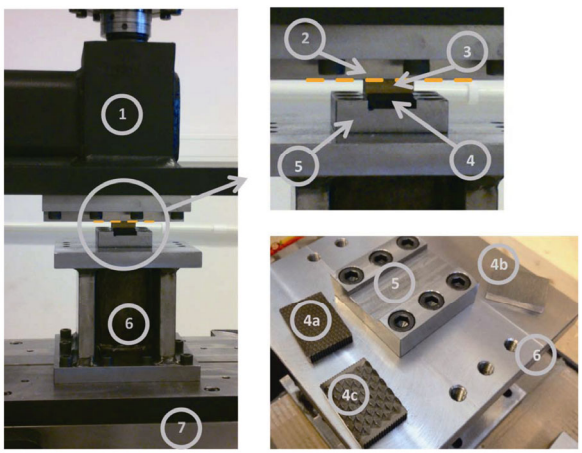

Fig. 1 Set-up of the test with (1) upper cross-head for vertical movement, (2) exchangeable sliding plate, (3) test specimen, (4a–4c) exchangeable mounting plates, (5) fixture, (6) lower loading device, and (7) lower sledge for horizontal movement; the sliding plane is shown in orange.

The sliding plate (part 2) was 175 mm long and 32 mm wide between the mounting screws. The mounting was exchangeable to enable plates with different surface finish to be fitted easily. The sliding plates were cleaned with acetone before each test to eliminate residues from the previous test. The specimens and the mounting plates were mounted in the machine to ensure that the compressive load was acting in the vertical line of the vertical load cell.

2.2 Specimen preparation

LVL (Kerto®-S from Metsä Wood, Finland) was chosen as the wood material for the tests. First, bars with a cross section of 30 mm × 30 mm were cut from LVL-beams in the respective directions relative to the main direction (= grain direction). The 10-mm thick specimens to be tested were cut from the bars in the subsequent step and appropriately labelled to show their orientation (Fig. 2). The area of nominally 30 mm × 30 mm was subjected to friction. The material was stored in a climate chamber under standard conditions of 20 °C/65% RH before and after preparation.

2.3 Variations

Tests with variations in different parameters, such as vertical pressure, angle to the grain, moisture content of the LVL, and surface roughness of the steel plate, were performed. For some of the tests, cross-combinations were performed. Note that the angle to grain refers to the angle between the normal load and the grain direction in the test specimen, and that in all tests, the sliding was parallel to the interlaminar bond lines of the LVL (Fig. 2).

The parameters are discussed separately and in detail as follows:

1) Pressure: The nominal compression loads in terms of pressure onto the surface were varied between 0.30 and 30 MPa. The pressure was applied by active control of the force on the specimen. The load levels were defined assuming a cross-sectional area of nominally 30 mm × 30 mm. Owing to slightly different dimensions of the specimens, all specimens were measured before testing to determine the actual applied pressure. Pressure variation was tested for

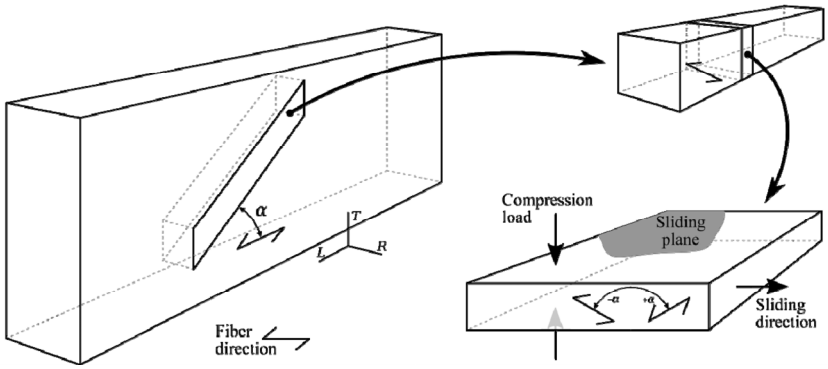

Fig. 2 Specimen preparation using an LVL beam (left) from which bars with a cross-section of 30 mm × 30 mm were cut out (top right) and subsequently the specimens for testing (bottom right), shown for arbitrary angles $\pm\alpha$ to the grain direction.

fiber angles 0° and 90° with different stepping depending on the angle to the grain (as shown in Table 1).

The maximum values for the applied compression loads are lower than the corresponding maximum compression strength for uniaxial loading of the LVL pieces. At high pressures, there is a risk for the specimens notwithstanding the combined loading by compression and shear.Thus, only two specimens could be tested for a load of 10 MPa at 90° fiber direction, while failure before slipping occurred in the other specimens of this series.

2) Plate roughness: Two different types of surface roughness were tested for the sliding between steel and wood. The standard steel surface, used for most of the tests, was polished whereas the second surface was roughened using sandblasting. The steel material was identical for both plates. The roughness parameters *Ra* and *Rq* were determined as 0.66 μm and 0.83 μm for the polished surface and as 6.38 μm and 8.15 μm for the sand-blasted surface, respectively. Depending on the angle to the grain, different normal pressures were applied (as shown in Table 2).

3) Moisture content: The basic variation was defined under standard climatic conditions of 20 °C/65% RH. Additionally, tests on wet and dry specimens were performed (as shown in Table 3). For the wet specimens, rods were stored by submerging in water for several days before cutting the specimens from them. In addition, the individual specimens were submerged in water again for some hours to ensure they were soaked before testing. Finally, water was poured onto the specimen surface facing the sliding plate. The dry specimens were put into an oven at 105 °C for approximately 24 h before testing.

Subsequently, the specimens were individually removed from the oven before testing to avoid re-uptake of moisture from the surrounding air.

Table 1 Test conditions for tests with varied nominal pressure.

Nominal pressure (MPa)	Fiber direction	Plate roughness	Moisture content
0.30, 1.0, 10.0, 30.0	0°	polished	20 °C/65% RH
0.30, 0.60, 1.0, 2.50, 5.0, 7.5, 8.5, 10.0	90°	polished	20 °C/65% RH

Table 2 Test conditions for tests with varied roughness of the steel plate.

Nominal pressure (MPa)	Fiber direction	Plate roughness	Moisture content
0.30, 5.00	0°	polished, rough	20 °C/65% RH
0.30, 1.66	+/-45°	polished, rough	20 °C/65% RH
0.30, 1.00	90°	polished, rough	20 °C/65% RH

Table 3 Test conditions for tests with varied moisture content

Nominal pressure (MPa)	Fiber direction	Plate roughness	Moisture content
0.30	0°	polished	20 °C/65% RH, wet, dry
5.00	0°	polished	wet, dry
30	0°	polished	20 °C/65% RH, dry
0.30, 1.00, 2.50	90°	polished	20 °C/65% RH, wet, dry
8.50	90°	polished	20 °C/65% RH, dry

The actual moisture contents of the wet and dry specimens were not measured specifically.

4) Angle-to-the-grain: The rods were cut at different angles to the grain direction. Thus, specimens with grain angles of 0°, +/-15°, +/-30°, +/-45°, +/-60°, +/-75°, and 90° were prepared (as shown in Table 4). This should inform whether the coefficients of friction differ and if the grain angle is acting against or with the shear surface. Specimens at all angles were tested at 0.30 MPa pressure as well as at a higher-pressure level. Because compressive strength significantly depends on load-to-grain angle, the upper pressure level was approximated by the Hankinson formula [20], assuming a strength value of 30 MPa for compression parallel to the grain (0°) and one of 5 MPa for compression perpendicular to the grain (90°) testing at standard conditions (the interaction curve is shown in Fig. 3).

2.4 Test procedure

Automated procedures could be employed for executing each test and measuring forces and displacements. Figure 4 shows the standard procedure for loading and testing. In the first step, a vertical load was applied (using different displacement rates) while, simultaneously, the horizontal sledge was controlled by the control system of the testing machine to enable horizontal movement, thereby preventing any horizontal load. A halting phase of 30 s was introduced to allow for possible creep deformations to decay (with the desired load kept constant).

Table 4 Test conditions for tests with varied angle-to-the-grain.

Nominal pressure (MPa)	Fiber direction	Plate roughness	Moisture content
0.30	0°, +/-15°, +/-30°, +/-45°, +/-60°, +/-75°, 90°	polished	20 °C/65% RH
30, 22.5, 13.3, 8.6, 6.3, 5.3, 5	0°, +15°, +/-30°, +/-45°, +/-60°, +/-75°, 90°	polished	20 °C/65% RH

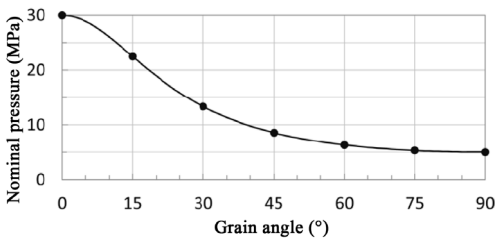

Fig. 3 Nominal upper compression stress level for varying grain angles.

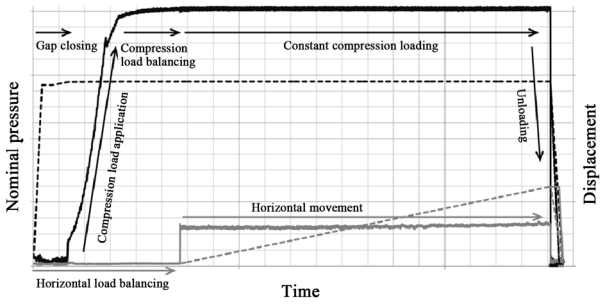

Fig. 4 Schematic presentation of the procedure showing the sequence of vertical loading, load balancing and the constant compression loading as well as horizontal load balancing and horizontal movement in sliding direction, followed by the unloading at test end (forces in full and displacements in dashed lines with the vertical direction in black and the horizontal direction in grey, respectively).

Thereafter, the horizontal sledge was moved at a rate of 10 mm/min while the vertical load was held constant. The horizontal force developed rapidly until the point where the specimen started to slip relative to the steel surface. Horizontal movement continued for a total horizontal displacement of 30 mm. In case the specimen failed, the test was aborted prematurely.

Data logging was set to a rate of 5 Hz during the initial stage, while a frequency of 256 Hz was chosen in the time range from the onset of horizontal movement and 5 seconds onwards.

Using this high rate of data acquisition, the zigzag shaped load curves, indicating a stick-slip behavior, could be monitored adequately. Subsequently, at the stage of more continuous movement, a lower logging frequency of 20 Hz was chosen. μ

2.5 Evaluation procedure

The acquired data was evaluated using a MATLAB® script. First, the raw data was checked for integrity, and the ratio of horizontal to vertical force, F_h/F_v, was determined. The area where the force ratio increased steeply was studied in detail. Ideally, the force ratio peaks at a single point before it switches into a zigzag-shaped curve, which is typical for a

stick-slip behavior of sliding friction. It was assumed that the beginning of the stick-slip region in the force ratio curve was the point at which the coefficient of static friction, μ_f, could be determined.

In some tests, the force ratio curves are observed to decrease with slip length. This is the generally assumed behavior of objects sliding on each other, with a peak value representing the static coefficient of friction μ_f, and a lower value representing the coefficient of sliding friction μ_s, i.e., $\mu_f > \mu_s$. In other tests, the ratios between the normal and the shear forces are approximately constant or even increasing (i.e., $\mu_f \leqslant \mu_s$). Because sliding friction is not focused in this study, this behavior is not further analyzed and discussed.

Not all specimens behaved as ideally presumed, and a semi-automated procedure was deployed to determine the coefficient of friction. The coefficients of friction were manually marked in MATLAB diagrams of the test data; thereafter, the MATLAB script automatically wrote the result to a database. The following statistical evaluation (determination of mean values and standard deviation) was performed automatically.

The load-slip curves did not always follow an ideally expected behavior as described above; hence, manual selection of the friction coefficient was easier to accomplish than creating a fully automated evaluation process. Examples of this behavior include tests that did not show a clear single peak but a more gradual transition to a plateau value (particularly observed when high forces were involved) or when an initial slip was observed that could be attributed to compliance in other parts of the set-up, which were thus neglected.

The cross-section area of the sliding plane does not fit into the equation. Therefore, the dimensions of the specimens are not necessarily required for determining the coefficient of friction. Nevertheless, to compare the results for different load levels, the actual applied pressure is determined from the applied load and the dimensions of the specimens. The figures in the subsequent section show the actual applied pressure level (mean value of the specimens in the series), and the tables present the nominal and actual pressure level (mean value of the specimens in the series). Differences between the nominal and the actual pressure level can be found throughout the tests with the actual value being approximately about 5%–10% higher.

3 Results

The coefficient of friction was determined separately for each specimen. A statistical evaluation was conducted to quantify the scattering of the results. The measurements are summarized in the following figures and tables.

In the figures, the quartile values and the mean values are plotted (grey line). Additionally, whiskers are added, which represent the maximum and minimum values within each series.

In the tables, the mean values are listed together with the standard deviation for each variation. For information, the number of specimens as well as the nominally and the actually applied pressure level (mean value of the specimens) are provided.

3.1 Variation with pressure

For the standard conditions at 0° load angle, a clear influence of pressure on the coefficient of friction was found. At the lowest pressure of 0.32 MPa, the coefficient was found to be 0.24 and decreased to 0.18 when the load was increased (to 1.07 MPa). For higher loads, the coefficient remained stable at approximately 0.17 for pressure levels of 10.60 and 31.84 MPa. Contrarily, the coefficient of friction for testing at 90° to the fiber showed less variation with pressure. Starting at 0.18 for the lowest pressure level, it dropped slightly to approximately 0.16 at a pressure of 1.07 MPa and increased again to approximately 0.17 at higher pressure levels. Note that while the coefficient of friction for 0° is higher at low loads compared to testing at 90°, it becomes small for applied high-pressure levels. Figure 5 and Table 5 summarize the values.

The variance within each series (defined as the difference between the maximum and minimum of the measured values) was approximately constant for the tests at 0° with about one tenth of the respective mean values. For tests at 90° to the fiber,

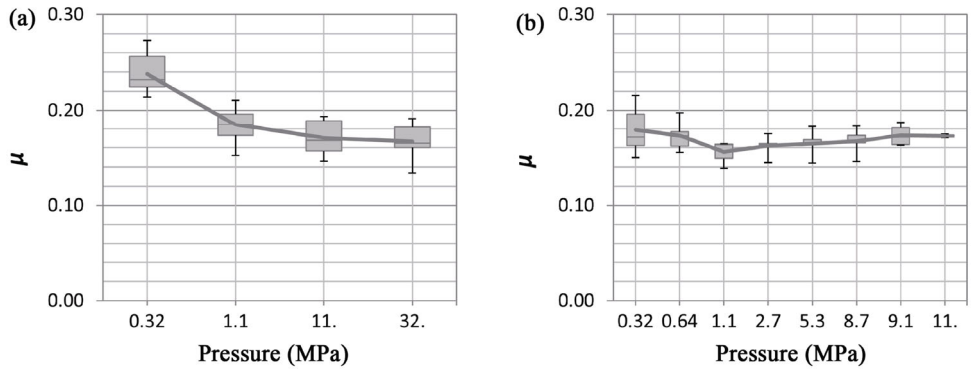

Fig. 5 Variation with pressure at (a) 0° and (b) 90° to the fiber.

Table 5 Mean value and standard deviation of μ for the variation with pressure at 0° (top) and 90° to the fiber (bottom).

Nominal pressure (MPa)	0.30	—	1.00	—	—	—	—	10.00	30.00
Actual pressure (MPa)	0.32	—	1.07	—	—	—	—	10.60	31.84
μ	0.238	—	0.184	—	—	—	—	0.170	0.167
Standard deviation of μ	0.021	—	0.018	—	—	—	—	0.018	0.019
Number of specimens	10	—	10	—	—	—	—	10	8
Nominal pressure (MPa)	0.30	0.60	1.00	2.50	5.00	7.50	8.50	10.00	—
Actual pressure (MPa)	0.32	0.64	1.07	2.66	5.35	8.67	9.10	10.74	—
μ	0.179	0.173	0.156	0.162	0.165	0.167	0.173	0.173	—
Standard deviation of μ	0.027	0.016	0.012	0.011	0.014	0.014	0.012	0.003	—
Number of specimens	5	5	5	5	5	5	4	2	—

the variance was approximately 10% of the respective mean values, with the exemption of tests at the lowest and the highest pressure level.

3.2 Variation with plate roughness

The roughness of the steel surface that the LVL was pressed onto evidently had a considerable influence on the coefficient of friction. All tested variations (different pressure levels and load angles) showed significantly higher coefficient of friction when using the rough surface than the smooth surface. For the lowest load level, at high roughness, the values were 3.4 and 3.7 times higher for the 0° and 90° load directions, respectively, than the smooth plate (coefficients of friction were 5.8 and 4.8 times higher at angles +45° and –45°, respectively). There was similar increase of 3.7 times at the higher load level of 1.0 MPa nominal pressure for the 90° load direction. Figure 6 and Table 6 summarize the values.

Moreover, with increased pressure level, the coefficients decreased, resembling the smooth plate. Due to the high values, the maximum possible pressure level was significantly lower than for the smooth plate. Increasing the applied pressure would cause a combined crushing/shear failure of the specimen when the shear stress developed.

3.3 Variation with moisture content

An increase in the coefficient of friction with increased moisture content of the specimen was observed. At 0°, the coefficient of friction increased by approximately 74% at 0.30 MPa nominal pressure level and more than double (+123%) at 5 MPa nominal pressure level when changing from dry to wet state. There was no change observed between the dry and the standard state for the pressure level of 30 MPa (the wet state could not be tested for this pressure level). Figure 7 and Table 7 summarize the values.

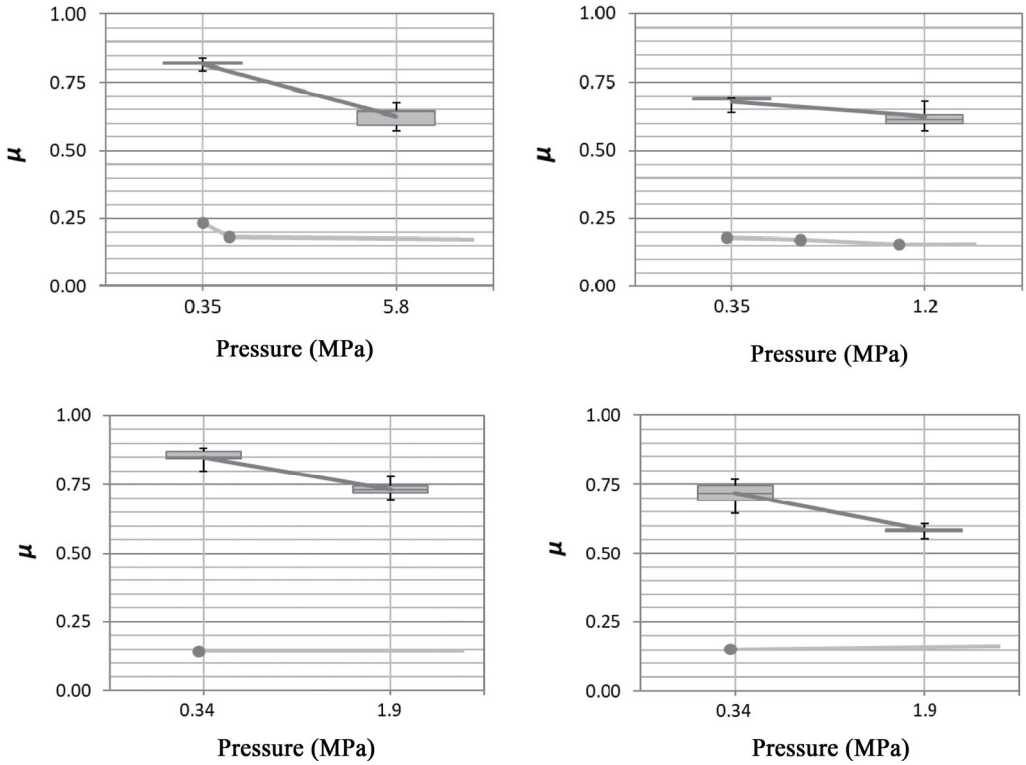

Fig. 6 Variation with plate roughness at 0° and 90° (top row) and □45° and +45° (bottom row) to the fiber (from left to right) for different pressure levels (the light lines with lower values are the corresponding values for the polished steel plate).

Table 6 Mean value and standard deviation of μ for the variation with high roughness of the steel plate at 0°, +/-45°, and 90° to the fiber at different pressure.

Angle to the grain (°)	0	0	–45	–45	+45	+45	90	90
Nominal pressure (MPa)	0.30	5.00	0.30	1.66	0.30	1.66	0.30	1.00
Actual pressure (MPa)	0.35	5.81	0.34	1.90	0.34	1.90	0.35	1.18
μ	0.818	0.626	0.851	0.733	0.719	0.586	0.680	0.624
Standard deviation of μ	0.017	0.042	0.032	0.032	0.038	0.014	0.024	0.035
Number of specimens	5	5	5	5	5	5	5	5

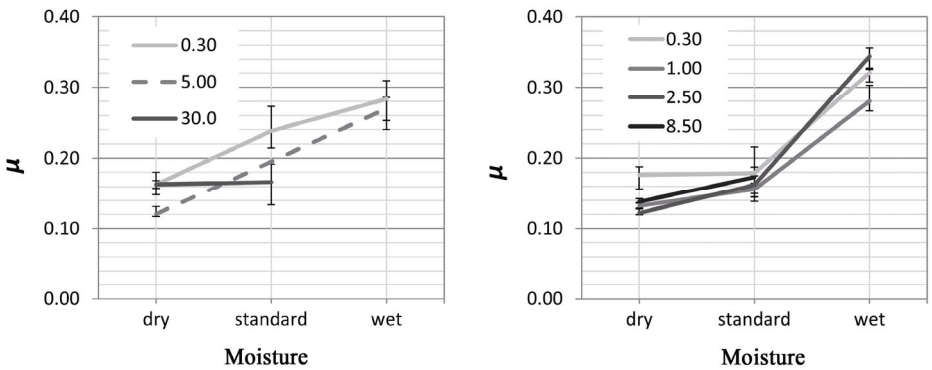

Fig. 7 Variation with moisture content at 0° (left), and 90° to the fiber (right) for different pressure levels.

Table 7 Mean value and standard deviation of μ for the variation with moisture content at different pressure for 0° (top) and 90° to the fiber (bottom).

Moisture content	dry	std	wet	dry	std	wet	dry	std	wet	—	—	—
Nominal pressure (MPa)	0.30	0.30	0.30	5.00	—	5.00	30.00	30.00	—	—	—	—
Actual pressure (MPa)	0.35	0.32	0.35	5.88	—	5.79	34.85	31.84	—	—	—	—
μ	0.163	0.238	0.283	0.121	—	0.270	0.163	0.167	—	—	—	—
Standard deviation of μ	0.013	0.021	0.022	0.006	—	0.017	0.005	0.019	—	—	—	—
Number of specimens	4	10	5	5	—	5	5	8	—	—	—	—
Moisture content	dry	std	wet	dry	std	wet	dry	std	wet	dry	std	wet
Nominal pressure (MPa)	0.30	0.30	0.30	1.00	1.00	1.00	2.50	2.50	2.50	8.50	8.50	—
Actual pressure (MPa)	0.34	0.32	0.35	1.13	1.07	1.15	2.83	2.66	2.93	9.59	9.10	—
μ	0.176	0.179	0.321	0.132	0.156	0.280	0.122	0.162	0.344	0.138	0.173	—
Standard deviation of μ	0.012	0.027	0.008	0.003	0.012	0.014	0.003	0.011	0.012	0.003	0.012	—
Number of specimens	5	5	5	5	5	5	5	5	5	4	4	—

At 90°, the increase from the dry to the wet state was similarly high with +82%, +112%, and +182% for the nominal pressure levels of 0.30, 1.00, and 2.50 MPa, respectively. However, at the highest pressure level, the wet state could not be tested. The increase from the dry to the standard state was considerably low, which was almost negligible at 0.30 MPa.

With one exemption, the coefficient of variation within each series was constantly lower than 10%.

3.4 Variation with angle-to-the-grain

The highest coefficient of friction was observed at 0° grain angle. The coefficients decreased with high grain angle, showing a minimum at +/-30°, and then increased again towards 90° angles (but did not reach the high values obtained at 0°). Note that there was a significant decrease in the coefficient of friction immediately after the grain angle deviated by only 15° from loading parallel to the grain, indicating a high sensitivity at approximately 0°. This is similar to the high sensitivity of other wood properties, such as stiffness and strength, if the load direction deviates around the fiber direction. Figure 8 and Table 8 summarize the values.

A variation with fiber angle was not clear for the tests at high pressure level; the coefficients determined were rather constant. Mean values ranged between 0.136 and 0.197, and most variations were lower than the corresponding values at high friction. The coefficients for +30° and +45° exhibited a high value; a high variation was reported for +60°. However, the data for –15° is missing owing to a mistake during testing; thus, the results could not be used.

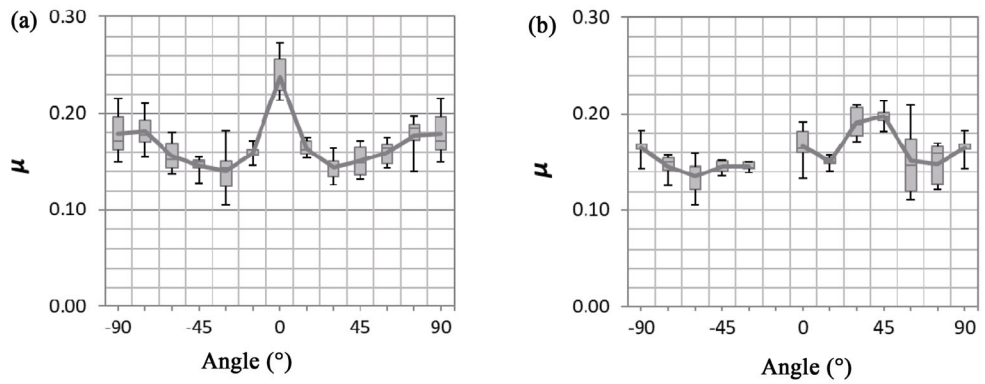

Fig. 8 Variation with angle-to-the-grain for (a) low pressure level and (b) high pressure level.

Table 8 Mean value and standard deviation of μ for the variation with angle-to-the-grain at low (top) and high pressure (bottom).

Angle to the grain (°)	–90	–75	–60	–45	–30	–15	0	+15	+30	+45	+60	+75	+90
Nominal pressure (MPa)	0.30	0.30	0.30	0.30	0.30	0.30	0.30	0.30	0.30	0.30	0.30	0.30	0.30
Actual pressure (MPa)	0.32	0.34	0.34	0.34	0.34	0.34	0.32	0.34	0.34	0.34	0.34	0.34	0.32
μ	0.179	0.181	0.156	0.146	0.141	0.159	0.238	0.164	0.145	0.151	0.160	0.177	0.179
Standard deviation of μ	0.027	0.021	0.017	0.011	0.029	0.009	0.021	0.009	0.015	0.017	0.013	0.025	0.027
Number of specimens	5	5	5	5	5	5	10	5	5	5	5	4	5
Angle to the grain (°)	–90	–75	–60	–45	–30	–15	0	+15	+30	+45	+60	+75	+90
Nominal pressure (MPa)	5.00	5.30	6.30	8.60	13.3	—	30.0	22.5	13.3	8.60	6.30	5.30	5.00
Actual pressure (MPa)	5.35	6.01	7.13	9.83	15.2	—	31.8	25.6	15.2	9.86	7.21	6.05	5.35
μ	0.165	0.146	0.136	0.146	0.146	—	0.167	0.151	0.191	0.197	0.152	0.149	0.165
Standard deviation of μ	0.014	0.014	0.022	0.007	0.005	—	0.019	0.006	0.017	0.012	0.040	0.022	0.014
Number of specimens	5	4	5	5	5	—	8	5	5	5	5	5	5

4 Discussion and conclusions

Coefficients of friction were determined for LVL on steel surfaces; particularly, the effects of high-pressure levels in the shear plane were studied.

The experiments showed a large variation within each tested series. This justifies that friction is highly dependent on the actual conditions of the surfaces in contact with, for instance, the properties of the wood matrix highly vary within a short range. Additionally, the cutting processes influence the texture of the formed surface.

Nevertheless, the wide range of the tested variations allows selecting more or less influencing parameters together with a range of friction values to be expected for the respective variation. Within the studied variations, the varied surface roughness of the steel plate has the highest influence. The coefficients recorded on the rough steel surface were up to 0.82, approximately 3.5 times the value for friction on smooth steel surfaces.

High moisture content samples resulted in significantly higher coefficients than the oven-dry or conditioned samples. Wet specimens, tested by applying pressure perpendicular to the fiber, resulted in coefficients of more than 0.30, while samples tested by applying pressure parallel to the fiber was slightly below 0.30. Differences between standard conditions and oven-dry specimens were moderate but noticeable for tests where pressure was applied perpendicular to the fiber.

Mixed conclusions are drawn for the dependence owing to pressure load-to-fiber direction. For low load levels, the highest coefficient of friction (0.24) is found at 0° fiber direction relative to the applied pressure, with a distinct decrease when tested at +/-45°, which marked the lowest coefficients (0.15). For tests where the pressure was applied at 90°, coefficients of friction were slightly high at 0.18. At high load levels, the differences owing to load direction were less obvious, mainly because of significantly lower coefficients for cases where pressure was applied parallel to the fiber. From a phenomenological perspective, it could be argued that the influence of small variations in the surface roughness of the wood and possibly the influence of grain angle are expected to be small for high pressure levels owing to homogenization of the surface by local plastic deformation. Ezzat, Hasouna, and Ali [21] made similar conclusion when observing a reduction of coefficient of friction when increasing applied pressure in the study of friction on polymeric indoor flooring material.

When pressure was applied parallel to the fiber, a clear dependence on the amount of pressure is found with high coefficients, 0.24, at lower pressure levels and flattening out at 0.17 for high pressure levels (a reduction by 30%). Small differences were obtained when load was applied perpendicular to the grain; nevertheless, a reduced coefficient of friction is obtained with increased pressure.

The previous studies mostly used clear wood

and not LVL as the studied material. However, qualitative conclusions are drawn that fit to the obtained data. The comparably high coefficients found, e.g., in the study by Bejo, Lang and Fodor [15], may be interpreted as an extension of the present study to even low applied pressure levels. Consequently, the coefficients of friction would be highly dependent on the applied load level whereby values of up to 1.20 are encountered with almost no applied pressure (e.g., in Ref. [12]). A rapid drop-off for moderate pressure levels is found, and thereafter, only small changes towards high pressure levels are observed. Therefore, strict differentiation between low and high loaded interfaces is required.

In practical applications, the role of friction is overlooked and the consequences are difficult to quantify. Additionally, the surface conditions of steel and wood surfaces may change over time because of moisture (rust on the steel plate, swelling and shrinking of the wood) or biological activities (decay of the wood surface). This can cause severe alterations of the contact properties and the friction between them, as well as significant changes to the pressure acting on the shear plane.

Finally, the use of realistic values for coefficients of friction in numerical simulations is necessary. Both inappropriately high and low coefficients of frictions are encountered in simulations, which are not realistic for the specific field (see the section on dowel-type connections in timber engineering in the introduction). Locally, friction often plays a significant role in the transfer of loads between structural parts. Thus, choosing the wrong coefficients may cause misinterpretations of the results, as well as "adjustments" of the results. Therefore, we agree with Ju and Rowlands [8] who reported that ignoring the effects of friction does not necessarily create a more conservative design by increasing stresses in the structure and the role of friction should further be studied.

References

[1] Hirai T, Meng Q, Sawata K, Koizumi A, Sasaki Y, Uematsu T. Some aspects of frictional resistance in timber construction. In *10th World Conference on Timber Engineering*, Asahikawa, Japan, 2008: 140–147.

[2] Dorn M. Investigations on the serviceability limit state of dowel-type timber connections. Ph.D Thesis. TU Wien, 2012

[3] Sjödin J, Serrano E, Enquist B. An experimental and numerical study of the effect of friction in single dowel joints. *Holz Roh Werkst* **66**: 363–372 (2008)

[4] Dorn M, de Borst K, Eberhardsteiner J. Experiments on dowel-type timber connections. *Eng Struct* **47**: 67–80 (2012)

[5] De Borst K, Jenkel C, Montero C, Colmars J, Gril J, Kaliske M, Eberhardsteiner J. Mechanical characterization of wood: An integrative approach ranging from nanoscale to structure. *Comput Struct* **127**: 53–67 (2013)

[6] Sandhaas C. Mechanical behaviour of timber joints with slotted-in steel plates. Ph.D Thesis. Technische Universiteit Delft, 2012

[7] C. Sandhaas and J.W.G. van de Kuilen. Material model for wood. *Heron*, **58**, 2013.

[8] Ju S H, Rowlands R E. A three-dimensional frictional stress analysis of double-shear bolted wood joints. *Wood Fiber Sci* **33**: 550–563 (2001)

[9] Atack D, Tabor D. The friction of wood. *Proc Roy Soc A* **246**: 539–555 (1958)

[10] Klamecki B E. Friction mechanisms in wood cutting. *Wood Sci Technol* **10**: 209–214 (1976)

[11] Murase Y. Friction of wood sliding on various materials. *J Fac Agric Kyushu Univ* **28**: 147–160 (1984)

[12] Möhler K, Herröder W. The range of the coefficient of friction of spruce wood rough from sawing. *Holz Roh*

Werkst **37**: 27–32 (1979)
[13] Möhler K, Maier G. Der Reibbeiwert bei Fichtenholz im Hinblick auf die Wirksamkeit reibschlüssiger Holzverbindungen. *Eur J Wood Wood Prod* **27**: 303–307 (1969)
[14] McKenzie W M. Friction coefficient as a guide to optimum rake angle in wood machining. *Wood Sci Technol* **25**: 397–401 (1991)
[15] Bejo L, Lang E M, Fodor T. Friction coefficients of wood-based structural composites. *Forest Prod J* **50**: 39–43 (2000)
[16] Kuwamura H. Coefficient of friction between wood and steel under heavy contact — Study on steel-framed timber structures Part 9. *J Struct Eng* **76**: 1469–1478 (2011)
[17] Seki M, Sugimoto H, Miki T, Kanayama K, Furuta Y. Wood friction characteristics during exposure to high pressure: Influence of wood/metal tool surface finishing conditions. *J Wood Sci* **59**(1): 10–16 (2012)
[18] Seki M, Nakatani T, Sugimoto H, Miki T, Kanayama K, Furuta Y. Effect of anisotropy of wood on friction characteristics under high pressure conditions. (in Japan). *Zairyo/Journal of the Society of Materials Science* **61**: 335–340 (2012)
[19] ASTM G 115. Standard guide for measuring and reporting friction coefficients. ASTM, 2013.
[20] Hankinson R L. *Investigation of crushing strength of spruce at varying angles of grain*, Air Service Information Circular No. 259, 1921
[21] Ezzat F H, Hasouna A T, Ali W. Friction coefficient of rough indoor flooring materials. *JKAU: Eng Sci* **19:** 53–70 (2008)

Michael DORN. He received his Ph.D. in civil engineering from Vienna University of Technology in 2012. He joined Linnaeus University, Växjö, Sweden, in 2012 as a postdoc and later research assistant, since 2016 he is Associate Professor at Linnaeus University. His research interests include timber engineering in general, with composite structures, connections and structural health monitoring in particular. He works both with experimental and numerical methods.

Karolína HABROVÁ. She completed a M.Sc. degree in structural engineering at Linnaeus University, Sweden in 2014. She also received her master's degree in process engineering in 2016 from Czech University of Life Sciences, Prague. She has recently obtained her Ph.D. in material engineering at Czech University of Life Sciences, Prague. Her research areas cover material degradation, polymers, and composite materials.

Radek KOUBEK. He received his bachelor's degree and later master's degree in process engineering in 2013 and 2016, respectively, from the Czech University of Life Sciences, Prague. In between, he completed a M.Sc. degree in structurale Engineering at Linnaeus University, Sweden, in 2014. He is currently working as a consultant within air-conditioning in the UK.

Erik SERRANO. He received his Ph.D. in structural mechanics in 2001. During 2007–2014, he was professor of timber engineering at Linnaeus University, Växjö, Sweden, and since 2015 he is professor of structural mechanics at Lund University, Sweden. Fracture mechanics has been an important basis in his research work and topics covered include the mechanical behavior of wood, engineered wood products like glued laminated timber and cross laminated timber and mechanical and adhesive joints for wood-based applications. Professor Serrano is a member of the Royal Swedish Academy of Engineering Sciences (IVA).